Author Manuscript

Author Manuscript

Author Manuscript

Author Manuscript

HHS Public Access

Author manuscript

Chem Biol. Author manuscript; available in PMC 2016 March 19.

Published in final edited form as:

Chem Biol. 2015 March 19; 22(3): 355–368. doi:10.1016/j.chembiol.2015.02.003.

Activation of Muscular TrkB by its Small Molecular Agonist 7,8-Dihydroxyflavone Sex-Dependently Regulates Energy Metabolism in Diet-Induced Obese Mice

Chi Bun Chan[1,2], **Margaret Chui Ling Tse**[1,2], **Xia Liu**[1], **Shuai Zhang**[1], **Robin Schmidt**[1], **Reed Otten**[1], **Liegang Liu**[3], and **Keqiang Ye**[1,*]

[1]Department of Pathology and Laboratory Medicine, Emory University School of Medicine, 615 Michael Street, Atlanta, GA 30322, USA

[2]Department of Physiology, University of Oklahoma Health Sciences Center, 940 Stanton L. Young Boulevard, Oklahoma City, OK 73104, USA

[3]Department of Nutrition and Food Hygiene, Hubei Key Laboratory of Food Nutrition and Safety, School of Public Health, Tongji Medical College, Huazhong University of Science & Technology, 13 Hangkong Road, Wuhan, 430030, P.R. China

SUMMARY

Chronic activation of brain-derived neurotrophic factor (BDNF) receptor TrkB is a potential method to prevent development of obesity, but the short half-life and nonbioavailable nature of BDNF hampers validation of the hypothesis. We report here that activation of muscular TrkB by the BDNF mimetic, 7,8-dihydroxyflavone (7,8-DHF), is sufficient to protect the development of diet-induced obesity in female mice. Using in vitro and in vivo models, we found that 7,8-DHF treatment enhanced the expression of uncoupling protein 1 (UCP1) and AMP-activated protein kinase (AMPK) activity in skeletal muscle, which resulted in increased systemic energy expenditure, reduced adiposity, and improved insulin sensitivity in female mice fed a high-fat diet. This antiobesity activity of 7,8-DHF is muscular TrkB-dependent as 7,8-DHF cannot mitigate diet-induced obesity in female muscle-specific *TrkB* knockout mice. Hence, our data reveal that chronic activation of muscular TrkB is useful in alleviating obesity and its complications.

INTRODUCTION

Brain-derived neurotrophic factor (BDNF) is a member of the neurotrophin family, which plays an important role in synaptic plasticity, neuronal survival, development, and differentiation (Huang and Reichardt, 2001). Through activating its cognate receptor, the

© 2015 Elsevier Ltd All rights reserved

*Correspondence: kye@emory.eduhttp://dx.doi.org/10.1016/j.chembiol.2015.02.003.

AUTHOR CONTRIBUTIONS

C.B.C. and K.Y. designed the experiments; C.B.C., M.C.L.T., X.L., S.Z., R.S., and R.O. performed the experiments; C.B.C., L.L., and K.Y. analyzed the data; C.B.C. and K.Y. wrote the manuscript.

SUPPLEMENTAL INFORMATION

Supplemental Information includes five figures and three tables and can be found with this article online at http://dx.doi.org/10.1016/j.chembiol.2015.02.003.

Author Manuscript Author Manuscript Author Manuscript Author Manuscript

tropomyosin-related kinase receptor B (TrkB), BDNF triggers TrkB autophosphorylation to initiate several signaling cascades, including the PI3K/Akt, Ras/Raf/ERK, and PLCγ/PKC pathways (Numakawa et al., 2010). It has been reported that infusion of BDNF into the lateral ventricle suppresses food intake and body weight gain in rats (Pelleymounter et al., 1995). In both humans and mice, *BDNF/TrkB* ablation or mutation causes hyperphagia and obesity phenotype (Gray et al., 2006; Yeo et al., 2004; Kernie et al., 2000). Since selective depletion of the *BDNF* gene in the neurons of the ventral medial hypothalamus (VMH) and dorsomedial hypothalamus (DMH) is sufficient to induce hyperphagia and increase body weight gain in mice, it is also suggested that the hypothalamus is the major target site for BDNF to perform its anorexic activity (Unger et al., 2007). However, the specific action site of BDNF to inhibit food intake is mysterious as exogenous delivery of BDNF to the paraventricular hypothalamus (PVH), VMH, or medial nucleus tractus solitarius (mNTS) can all suppress calorie intake (Rios, 2013). Interestingly, administration of BDNF into *db/db* mice also transiently increases energy metabolism via an unclear mechanism (Nakagawa et al., 2000). Thus, manipulating BDNF/TrkB signaling may represent a potential strategy in combating or preventing the development of obesity. However, the beneficial role of chronic TrkB activation in preventing the development of long-lasting diseases such as obesity has not been tested because of the short half-life and nonbioavailable nature of BDNF (Poduslo and Curran, 1996), which hampers the development of a BDNF/TrkB-based therapeutic strategy.

To search for an orally bioavailable BDNF mimetic, we have identified 7,8-dihydroxyflavone (7,8-DHF) as a specific TrkB agonist, which induces TrkB dimerization and activation of its downstream signaling molecules, including Akt and ERK (Jang et al., 2010). Like BDNF, application of 7,8-DHF promotes the survival of cortical, hippocampal, retinal ganglion, and spiral ganglion neurons and prevents various oxidative or excitotoxicity-induced cell death in a TrkB-dependent manner (Jang et al., 2010; Gupta et al., 2013; Yu et al., 2013). Hence, 7,8-DHF can be applied to alleviate the syndromes of neurological disorders related to *BDNF* deficiency. For example, administration of 7,8-DHF enhances emotional learning, prevents the return of fear in extinction-trained mice (Baker-Andresen et al., 2013), prevents cognitive defects in a rat model of posttraumatic stress disorder (Andero et al., 2012), and elongates the lifespan and alleviates the pathological conditions of Rett syndrome (Johnson et al., 2012). 7,8-DHF also displays impressive therapeutic efficacy in animal models of Parkinson disease (Jang et al., 2010), Alzheimer disease (Zhang et al., 2013), and Huntington disease (Jiang et al., 2013). Furthermore, 7,8-DHF demonstrates a promising effect in enhancing axon regeneration in *BDNF* conditional knockout (cKO) mice but not in *TrkB* cKO mice (English et al., 2013). These studies strongly support that 7,8-DHF is a bioavailable TrkB agonist, which could be used as a molecular tool to study the beneficial role of chronic TrkB activation in diseases such as obesity.

We report here that chronic activation of TrkB by 7,8-DHF can be used as an effective method to prevent excess body weight gain during energy surplus. Moreover, we found that activation of muscular TrkB by 7,8-DHF is sufficient to ameliorate the development of

Author Manuscript Author Manuscript Author Manuscript Author Manuscript

obesity and its associated diabetes in female animals, suggesting peripheral TrkB signaling is equally important as that in the CNS to control systemic energy metabolism.

RESULTS

7,8-DHF Consumption Prevents the Development of Diet-Induced Obesity in Female Mice

In order to test if 7,8-DHF can control body weight, we included 7,8-DHF in the drinking water (final concentration 0.16 mg/ml) of C57BL/6 mice fed with chow or a high-fat diet (HFD, 45% kcal). 7,8-DHF administration did not cause significant toxicity or undesirable side effects as revealed by normal complete blood counts (Table S1) and tissue histology examinations (Liu et al., 2010). While female mice consuming 7,8-DHF displayed reduced body weight gain under HFD feeding, 7,8-DHF did not significantly decrease the body weight of mice fed with a chow diet (Figure 1A). Unexpectedly, 7,8-DHF was not effective in preventing body weight gain in male mice under HFD feeding either (Figure S1). Therefore, we performed the subsequent analyses in female mice only. HFD-fed female animals exhibited a drastic increase in inguinal white adipose tissue (WAT) mass, which was substantially reduced after 7,8-DHF treatment (Figure 1B). The adipocytes in 7,8-DHF-treated mice were also smaller (Figures 1C, lower panels, and 1D). Since 7,8-DHF stimulation did not inhibit adipogenesis in 3T3-L1 preadipocytes (Figure S2), the reduction in adipocyte size or mass is possibly a secondary effect of 7,8-DHF treatment. Circulating leptin (Figure 1E) and tumor necrosis factor alpha (TNFα) (Figure 1F) concentrations were also lower after 7,8-DHF treatment. Hepatic concentrations of cholesterol, triglyceride (TG), and free fatty acid (FFA) were significantly diminished in 7,8-DHF-treated animals under HFD feeding (Figures 1G–1I), which was in alignment with the reduced hepatic steatosis observed (Figure 1C, upper panels). Similarly, the TG and FFA concentrations in muscle were also decreased in the 7,8-DHF-treated animals (Figures 1H and 1I). Thus, treatment of mice with 7,8-DHF reduces diet-induced body weight gain and lipid accumulation in ectopic tissue.

7,8-DHF Treatment Improves Insulin Sensitivity and Glucose Tolerance

Insulin resistance is one of the most prominent complications of obesity. Since we found that 7,8-DHF is able to prevent diet-induced obesity, we then asked whether the treatment affects insulin sensitivity. 7,8-DHF treatment for 20 weeks significantly diminished fasting hyperglycemia in HFD-fed animals (Figure 2A). Obesity-induced hyperinsulinemia was also alleviated after 7,8-DHF consumption (Figure 2B), suggesting improved insulin sensitivity. Indeed, HFD-fed mice treated with 7,8-DHF revealed better glucose clearance during the glucose tolerance test (Figure 2C). We further examined systemic insulin sensitivity in 7,8-DHF-treated mice using the gold standard hyperinsulinemic-euglycemic clamp assay. As shown in Figures 2D and 2E, the glucose infusion rate was significantly higher in 7,8-DHF-treated mice than vehicle-treated animals, indicating an improved systemic insulin sensitivity. Insulin infusion also mediated higher hepatic glucose suppression and muscular glucose uptake in 7,8-DHF-treated mice (Figures 2F–2H). Concurring with these results, Akt phosphorylation was evidently higher in the liver and muscle of HFD-fed mice upon 7,8-DHF treatment, although upstream insulin receptor activity was not affected (Figures 2I and 2J). Hence, 7,8-DHF treatment mitigates obesity-induced insulin resistance.

Author Manuscript Author Manuscript Author Manuscript Author Manuscript

7,8-DHF Treatment Increases Energy Expenditure

Since BDNF is an anorexigenic factor that suppresses food intake, we next sought to determine if 7,8-DHF treatment could induce hypophagia. We found that mice fed with HFD and 7,8-DHF for 20 weeks contained less total body fat on body composition analysis (Figure 3A). Total lean mass was also decreased (Figure 3B). When fat and lean masses were normalized with total body weight, the percentage of lean body mass was comparable between the two treatment groups (52.6% ± 3.3% in the control group versus 59.0% ± 4.1% in the 7,8-DHF-treated group), whereas the percentage of fat mass was significantly reduced in 7,8-DHF-treated animals (27.0% ± 1.7% in the control group versus 19.6% ± 3.2% in the 7,8-DHF-treated group, $P < 0.05$, Student's t test, n = 6). To our surprise, total food intake at night was higher in mice after 7,8-DHF treatment (Figure 3C). On the other hand, total water uptake was prominently reduced in animals treated with 7,8-DHF (Figure 3D), probably because of the unfavorable taste of 7,8-DHF in the water. Locomotor activity was not changed after 7,8-DHF consumption (Figure 3E). Intestinal lipid absorption was comparable between the two groups, as the amount of residual lipid content in the feces was not significantly altered by 7,8-DHF (Figure S3). Presumably, the reduction in body weight in 7,8-DHF-treated mice under HFD feeding is not a result of decreased food intake or lipid absorption but enhanced energy metabolism. Indeed, both resting and nonresting energy expenditure were higher in the animals treated with 7,8-DHF (Figure 3F). Elevated oxygen consumption and carbon dioxide production were also detected after 7,8-DHF-treatment (Figures 3G and 3H), indicating an overall increase in metabolic rate after chronic 7,8-DHF consumption. On the other hand, the respiratory exchange ratio (RER) was not significantly changed in mice fed with HFD and 7,8-DHF, suggesting that the utilization balance between glucose and lipid was not affected (Figure 3I).

Gene Expression Analysis of 7,8-DHF-Treated Muscle and Liver

To dissect the molecular mechanisms underlying the antiobesity effect of 7,8-DHF, we performed a comprehensive analysis of the gene expression pattern in hindlimb skeletal muscle (a mixture of the soleus and gastrocnemius muscles) and liver of mice fed with HFD and 7,8-DHF. Microarray screening indicated that 22 hepatic genes were significantly upregulated and 14 hepatic genes were downregulated more than 2-fold in 7,8-DHF-treated liver when compared with the control group (Table S2). Of these genes, only two are related to energy or fatty acid metabolisms (Figure 4A; Table S2). The number of induced genes was much higher in the skeletal muscle after 7,8-DHF treatment. It was found that 58 muscle genes were significantly upregulated and 28 muscle genes were downregulated (Table S3). Twenty-three of these 86 genes are involved in glucose utilization, fatty acid oxidation, or energy production (Figure 4A; Table S3). Some of these genes, e.g. fatty acid elongase Elovl6 and bone morphogenetic protein 5 (Bmp5), have been reported to be important factors in regulating energy expenditure (Matsuzaka et al., 2007; Tseng et al., 2008). We validated the microarray findings by selectively testing those genes that have been reported in regulating glucose or fatty acid metabolism using real-time PCR. In agreement with the microarray data, expression of major urinary protein 1 (Mup1) (Zhou et al., 2009), perilipin 1 (Plin1) (Sztalryd et al., 2003), and the β subunit of cyclic AMP (cAMP)-dependent protein kinase type II (Prkar2b) (Cummings et al., 1996) was

Author Manuscript Author Manuscript Author Manuscript Author Manuscript

significantly higher in 7,8-DHF-treated muscle. On the other hand, 7,8-DHF-treated muscle expresses less mito chondrial NADH dehydrogenase 6 (ND6) (Bai and Attardi, 1998) than the control (Figure 4B). Interestingly, we found that expression of uncoupling protein 1 (UCP1), a mitochondrial protein that is responsible for nonshivering thermogenesis in brown adipose tissue (BAT) (Aquila et al., 1985; Cannon and Nedergaard, 2004), was robustly increased in the muscle of mice after 7,8-DHF treatment (Table S3; Figure 4C). The increased UCP expression was isoform specific as expression of other UCP isoforms (UCP2 and UCP3) was not altered in response to 7,8-DHF treatment (Figure 4C). We further confirmed the elevated UCP1 expression in 7,8-DHF-treated muscle using immunoblotting. As shown in Figure 4D, expression of UCP1 protein was specifically induced in the muscle of 7,8-DHF-treated mice but not in liver or WAT.

7,8-DHF Treatment Activates AMPK/ACC Signaling

Since ectopic UCP1 overexpression in skeletal muscle increases systemic energy expenditure and lipid utilization, leading to a reduction in gain of body weight of mice under HFD feeding (Li et al., 2000; Klaus et al., 2005; Neschen et al., 2008), we thus examined if the signal transduction pathway for lipid oxidation was also enhanced in 7,8-DHF-treated animals. HFD-fed mice with 7,8-DHF consumption displayed a significant increase in AMP-activated protein kinase (AMPK) phosphor-ylation in the muscle but not in the liver or WAT (Figure 5A, first panel). In line with this observation, phosphorylation of AMPK substrate acetylcoenzyme A carboxylase (ACC) was upregulated in the muscle (Figure 5A, third panel). ACC phosphorylation was also increased in liver and WAT. However, since the total amount of ACC was augmented in all tested tissues of 7,8-DHF-treated mice (Figure 5A, fourth panel), the ratio of phospho-ACC to total ACC was only significantly elevated in the muscle (Figure 5B, middle panel). Keipert et al. (2013) have reported that ERK phosphorylation was upregulated in the muscle of UCP1 transgenic mice, which is possibly a protective response to increased oxidative stress. We also observed that ERK phosphorylation was highly escalated in the liver and muscle of 7,8-DHF-treated mice (Figure 5A, fifth panel and Figure 5B). Interestingly, expression and phosphorylation of cAMP response element-binding protein (CREB), the transcription factor that controls UCP1 transcription (Rim and Kozak, 2002), were increased in liver, muscle, and WAT of 7,8-DHF-treated mice (Figure 5A, seventh and eighth panels). Thus, our immunoblotting analysis indicates that the lipid oxidation pathways are activated in the skeletal muscle of mice after chronic 7,8-DHF consumption.

Skeletal Muscle TrkB Is the Major Target of 7,8-DHF to Mediate its Antiobesity Effect

Although we observed that TrkB phosphorylation was increased in the hypothalamus of mice under chronic 7,8-DHF treatment (Figure S4), food intake was not suppressed in the 7,8-DHF-treated animals (Figure 3C), suggesting that the hypothalamus may not be the target tissue for 7,8-DHF to exert its antiobesity function. We thus hypothesized that muscle TrkB is the major target of 7,8-DHF for preventing the development of obesity under HFD feeding. We tested this hypothesis by feeding 7,8-DHF to genetically engineered mice with muscle-specific *TrkB* deletion. By mating transgenic mice that encompass two flox elements flanking the first coding exon of the *Ntrk2* gene and transgenic mice carrying a muscle creatine kinase (MCK)-promoter-driven Cre recombinase, we generated muscle-specific

Author Manuscript Author Manuscript Author Manuscript Author Manuscript

TrkB knockout (MTKO) mice (Figure 6A). Genomic (Figure 6B) and RT-PCR (Figure 6C) analyses confirmed the tissue-specific deletion of the *Ntrk2* gene in the skeletal muscle. Western blot analysis also indicated that the amount of TrkB protein was significantly reduced in the skeletal muscle of MTKO mice (Figure 6D). The residual signals in Figures 6C and 6D might result from the TrkB of the muscle-innervated sciatic nerve (Funakoshi et al., 1993). When female MTKO mice were fed with HFD and H_2O for 16 weeks, their body weight increased to the same extent as the wild-type (WT) animals; however, 7,8-DHF treatment significantly reduced body weight gain in WT but not MTKO mice (Figure 6E), although hypothalamic TrkB receptors could still be activated in MTKO mice (Figure S4). Moreover, no elevated AMPK and ACC phosphorylation was detected in 7,8-DHF-treated MTKO muscle, as the ratios of phosphoprotein/total protein remained comparable (Figures 6F and 6G). These results suggest that the muscle TrkB receptor is indispensable for 7,8-DHF to exert its antiobesity function.

7,8-DHF Increases Lipid Oxidation and UCP1 Expression in Cultured Muscle Cells

Our in vivo data indicate that 7,8-DHF might act on muscle TrkB to protect animals from developing diet-induced obesity. We further confirmed these results using an in vitro system. As expected, phosphorylation of TrkB and its downstream target Akt was increased in differentiated C2C12 myotubes upon 7,8-DHF treatment (Figure 7A), suggesting that TrkB signaling is intact in the C2C12 cells. In alignment with the in vivo data, increased AMPK and ACC phosphorylation was detected in 7,8-DHF-stimulated C2C12 myotubes in a time- (Figure 7B) and dose-dependent (Figure 7C) manner. Accordingly, 7,8-DHF stimulation caused a significant elevation of lipid oxidation in C2C12 myotubes (Figure 7D). Nevertheless, 7,8-DHF did not activate AMPK directly as the presence of 7,8-DHF did not enhance AMPK activities in the in vitro kinase assay (Figure S5). Inhibiting the kinase activity of TrkB using the specific inhibitor K252a (Tapley et al., 1992) diminished BDNF- or 7,8-DHF-induced AMPK and ACC phosphorylation (Figure 7E). On the other hand, C2C12 myotubes overexpressing TrkB displayed higher 7,8-DHF- or BDNF-induced AMPK and ACC phosphorylation (Figure 7F). We also found that 7,8-DHF decreased the cellular concentration of ATP and ADP (Figure 7G) but increased the ADP/ATP ratio (Figure 7H) in C2C12 myotubes. This elevation of the ADP/ATP ratio could be reduced in the presence of K252a (Figure 7I), suggesting that 7,8-DHF acts on TrkB to alter the concentration of cellular adenosine phosphate. Lastly, immunoblotting analysis validated that UCP1 expression and CREB phosphorylation in C2C12 were elevated after 7,8-DHF treatment (Figure 7J). Our results suggest that 7,8-DHF can directly alter the energy metabolism pathways in muscle cells.

DISCUSSION

Most studies on the antiobesity activity of BDNF/TrkB focus on their anorexic roles in the CNS, with little attention paid to other tissues, although both BDNF and TrkB mRNAs could be detected in peripheral organs such as muscle, pancreas, heart, kidney, and ovary (Shelton et al., 1995). In fact, BDNF synthesis in muscle cells is a dynamic process, which responds actively to exercise stimulation (Cuppini et al., 2007). Matthews et al. (2009) further demonstrated in vitro that stimulation of L6 muscle cells with BDNF enhanced

Author Manuscript Author Manuscript Author Manuscript Author Manuscript

AMPK activity via an unknown mechanism, suggesting that BDNF is a beneficial mediator of energy metabolism in muscle. Conceivably, activation of BDNF/TrkB signaling in muscle may provide a beneficial outcome to prevent obesity, but this hypothesis has not been proved in vivo because the nonbioavailable nature of BDNF and the tedious administration protocols do not favor any long-term study. Using the BDNF mimetic, 7,8-DHF, identified by our group, and MTKO mice, we have provided compelling in vivo evidence to support the idea that muscular TrkB is equally important to CNS TrkB in controlling body weight gain. We found that chronic administration of 7,8-DHF to mice ameliorates diet-induced obesity by activating the TrkB in muscle. Because the food intake and locomotor activities of the tested mice were not suppressed after 7,8-DHF treatment, together with the fact that 7,8-DHF consumption fails to protect MTKO mice from developing obesity under HFD feeding, we propose that 7,8-DHF acts on muscle tissue to enhance total energy expenditure. Indeed, our in vitro studies on C2C12 myotubes concur with the in vivo findings that 7,8-DHF stimulation elicits increased AMPK activity, lipid oxidation, and UCP1 expression. Presumably, activation of muscle TrkB by 7,8-DHF increases UCP1 expression, which results in an enhanced uncoupling reaction and a reduction in the cellular energy supply, leading to activation of AMPK and enhanced lipid oxidation, and eventually reduced body weight gain. Nevertheless, we could not exclude that other cascades, such as ERK signaling, are also involved in the antiobesity and antidiabetic action of 7,8-DHF because Fu et al. (2010) reported that dietary intake of genistein, a structurally related flavonoid, significantly improved hyperglycemia, glucose tolerance, and blood insulin levels in streptozotocin-induced diabetic mice via ERK activation. In short, our findings suggest that modulating muscle BDNF/TrkB signaling may represent a promising strategy for obesity therapy.

One of the key findings in the current study is that activation of the TrkB signaling in muscle leads to the expression of UCP1. UCP1 is a mitochondrial protein that disrupts the electrochemical gradient across the inner mitochondrial member, causing energy derived from oxidative phosphorylation to be released as heat (Cannon and Nedergaard, 2004). While this protein is highly expressed in BAT, ectopic expression of UCP1 in muscle enhances systemic energy expenditure (Klaus et al., 2005), elevates AMPK activation and lipid oxidation (Neschen et al., 2008), decreases muscle ATP and ADP content (Han et al., 2004), prevents the development of diet-induced obesity, and alleviates obesity-associated diabetes (Li et al., 2000). Total body lean mass is also reduced in *UCP1* transgenic mice, which is possibly a result of lower energy efficiency due to the enhanced uncoupling reaction (Klaus et al., 2005). These pheno-types in *UCP1* transgenic mice closely resemble our observations in mice fed with HFD and 7,8-DHF, which provides strong support for our conclusion that enhanced UCP1 is the key mechanism for the beneficial action of BDNF/TrkB signaling in muscular energy metabolism. Although the molecular mechanism of BDNF-induced UCP1 expression is unclear, promoter analysis suggested that the human UCP1 gene contains several cAMP responsive elements (del Mar Gonzalez-Barroso et al., 2000). Rim and Kozak (2002) further provide in vitro evidence that CREB controls *UCP1* transcription. Since CREB is one of the major downstream signaling molecules of the BDNF/TrkB pathway (Finkbeiner et al., 1997) and we also found that total expression as

Author Manuscript Author Manuscript Author Manuscript Author Manuscript

well as phosphorylation of CREB were upregulated in 7,8-DHF-treated muscle, it is reasonable to deduce that BDNF induces UCP1 expression in muscle via activating CREB.

Interestingly, 7,8-DHF treatment controls the development of obesity in a sex- and metabolic status-specific manner; only female animals under HFD feeding benefit from the BDNF mimetic compound. In alignment with our findings, subcutaneous injection of BDNF improves body weight gain and energy expenditure only in obese *db/db* but not in normal mice (Kernie et al., 2000). Sex dimorphism in the BDNF response is commonly observed in mice. For instance, change of body composition in female animals is more sensitive to BDNF as female *BDNF* cKO mice display a higher increase in body fat composition (Camerino et al., 2012). In addition, while male BDNF cKO mice exhibit hyperactivity but normal depression-related behaviors, female BDNF cKO mice display normal loco-motor activity but a striking increase in depression-like behavior (Monteggia et al., 2007). A recent study also reported that 7,8-DHF has more profound activity in protecting hypoxia ischemia-mediated neuronal death and white matter injury in female mice than in male mice (Uluc et al., 2013). The molecular mechanism for this sex dimorphism is unknown but it is suggested that the presence of sex-specific hormones may provide a possible explanation. For example, estrogen has been proposed to enhance BDNF functionality via crosstalking with TrkB signaling (Spencer et al., 2008). Presumably, these interacted sex-hormone-BDNF pathways are synergistic in female mice but are less relevant in determining the metabolic pheno-type in males.

Previous studies have reported that administration of BDNF into obese animals suppresses food intake via the hypothalamus (Wang et al., 2010). However, we did not observe any suppression of food intake in mice after chronic 7,8-DHF treatment. Rather, these animals display enhanced food intake. As such, 7,8-DHF may not act on hypothalamus neurons to control food intake as BDNF does. There are several explanations for these discrepant findings. First, the route of administration in our study is different from previous studies. In this report, 7,8-DHF was administrated to the animals via drinking water, and in some animals it will be metabolized in the gastrointestinal track or the liver (Liu et al., 2013), whereas BDNF administration in other studies was performed by either subcutaneous or intracerebral injections (Tsuchida et al., 2001). Since the brain clearance rate, diffusion rate, and metabolism may be different between BDNF and 7,8-DHF, the amount of 7,8-DHF that reached the hypothalamus in our study may not be high enough to trigger the same physiological response as BDNF. Alternatively, the cellular signaling events induced by BDNF and 7,8-DHF may be different although both of them are TrkB agonists. It is possible that activation of TrkB by BDNF or 7,8-DHF may induce differential receptor phosphorylation patterns, thus leading to the inducer-specific cellular response. Collectively, our results identify that the BDNF/TrkB signaling pathway in muscle controls lipid oxidation and energy expenditure and that the use of the BDNF mimetic 7,8-DHF displays great potential in treating obesity.

SIGNIFICANCE

Obesity is a major risk factor for a number of diseases including diabetes, cardiovascular diseases, liver steatosis, and even certain types of cancer. The increasing prevalence of

Author Manuscript Author Manuscript Author Manuscript Author Manuscript

obesity thus puts tremendous pressure on public health and economic systems. Although a considerable amount of work has been invested in developing new medications for obesity treatment, only a few effective pharmacotherapy strategies are available on the market. Chronic activation of TrkB is a potential method to treat or prevent obesity, but the hypothesis has not been validated because of the short half-life and nonbioavailable nature of BDNF. Using the BDNF mimetic, 7,8-DHF, as the molecular probe, we found that chronic activation of muscular TrkB modulates cellular energy expenditure and prevents the development of excess body weight gain in female mice under energy surplus. These results reveal the molecular mechanism of TrkB-regulated cellular energy metabolism and prove that chronic activation of muscular TrkB by 7,8-DHF can be used as a potential strategy against the development of obesity.

EXPERIMENTAL PROCEDURES

Animal Experiments

C57BL/6J mice were obtained from Jackson Laboratory. Eight-week-old animals were used in our experiments. Mice were housed in environmentally controlled conditions with a 12-hr light/dark cycle and had free access to standard rodent pellet food and water. The animal protocols were approved by the Institutional Animal Care and Use Committee (IACUC) of Emory University or Vanderbilt University. Animal care was given in accordance with institutional guidelines.

Blood glucose levels were measured by ACCU-CHEK Advantage Blood Glucose Meter (F. Hoffmann-La Roche). Serum insulin and leptin were measured by ELISA (Crystal Chem). Cholesterol, TG, and FFA levels in tissues or serum were measured using the Cholesterol/Cholesteryl Ester Quantitation Colorimetric Kit, Triglyceride Quantification Colorimetric Kit, and Free Fatty Acid Quantification Colorimetric Kit, respectively (BioVision). Serum TNFα was measured by ELISA (BD Biosciences). A glucose tolerance test was performed on mice after peritoneal injection of D-glucose (2 g/kg of body weight).

Generation of MTKO Mice

MTKO mice were generated by mating transgenic mice that encompass two flox elements flanking the first coding exon of Ntrk2 gene and transgenic mice carrying an MCK-promoter-driven Cre recombinase (Jackson Laboratory) until homozygosity. Genotyping was performed by PCR using genomic DNA isolated from the tail tip. PCR was performed using a combination of primers 5′-ACACACACAGTATATTTTACC-3′ (forward) and 5′-CAAGAAGTCAGAGACCAGAGAGA-3′ (reverse) for TrkB flox allele; and 5′-CCTGGAAAA TGCTTCTGTCCGTTTGCC-3′ (forward) and 5′-CCTGGAAAATGCTTCTGTCCGTTTGCC-3′ (reverse) for Cre transgene.

Chemicals and Reagents

C2C12, 3T3-L1, and HEK293 cells were purchased from ATCC and maintained as instructed. Differentiation of C2C12 was performed as reported (Burattini et al., 2004). Transfection in C2C12 was performed using DharmaFECT1 as instructed (Thermo Scientific). 7,8-DHF was purchased from Tokyo Chemical Industry. HFD (40% kcal) was

Author Manuscript Author Manuscript Author Manuscript Author Manuscript

obtained from Research Diet. Human insulin was obtained from Eli Lilly. Other chemicals were purchased from Sigma-Aldrich. Antibodies against pAkt S473, IR, pIR Y1150/1151 (#3024), pAMPKa T172 (#2535), AMPKα (#2603), pACC S79 (#3661), ACC (#3676), pERK T202/ Y204 (#9106), ERK (#9102), pCREB S133 (#9198), CREB (#4820), and TrkB (4603) were purchased from Cell Signaling. Anti-Akt1 (sc5298) and anti-pTrkB Y706 (sc135645) antibodies were obtained from Santa Cruz Biotechnology. Anti-UCP1 antibody (ab155117) was obtained from Abcam. Anti-tubulin antibody (T6074) was obtained from Sigma-Aldrich.

Western Blot Analysis

Tissues or cells were homogenized in lysis buffer containing 50 mM Tris (pH 7.4), 40 mM NaCl, 1 mM EDTA, 0.5% Triton X-100, 1.5 mM Na_3VO_4, 50 mM NaF, 10 mM sodium pyrophosphate, 10 mM sodium β-glycerophosphate, 1 mM phenylmethylsulfonyl fluoride, and 1× protease inhibitor cocktail (Sigma-Aldrich). Cell debris was removed by centrifugation and the supernatant (cleared cell lysate) was collected for immunoblotting. Western blot results were visualized using Pierce ECL Western Blotting Substrate (Thermo Scientific).

Microarray Analysis

Global gene expression in the hindlimb skeletal muscle (a mixture of soleus and gastrocnemius muscles) and liver tissues was performed using GeneChip Mouse Gene 1.0 ST Arrays (Affymetrix) as instructed. Results were analyzed by the computer program GenePattern (Reich et al., 2006).

RT-PCR

Total RNA was prepared by Trizol Isolation Reagent (Invitrogen). First-strand cDNA from total RNA was synthesized using Superscript III reverse transcriptase (Invitrogen) and oligo-dT_{17} as primer. Expression of Mup1 (F: CAA AAC AGA AAA GGC TGG TGA; R: GTT TTA CAA ACT TTT CCT TGA), Plin1 (F: AGA GTT CTG CAG CTG CCT GTG, R: CAG AGG TGC TTG CAA TGG GCA), Prkar2b (F: CCG TAT GGG CAG ATT GAG TA, R: CTA CTA AAT ACA AAC AAC AAA AAC CCT), ND6 (F: ATT AAA CAA CCA ACA AAC CCA C, R: TTT GGT TGG TTG TCT TGG GTT), and β-actin (F: AAC CGT GAA AAG ATG ACC CAG AT, R: CAC AGC CTG GAT GGC TAC GT) was detected using RealMasterMix SYBR ROX (5 Prime) on an ABI7500 Real-Time PCR System (Applied Biosystems). TrkB expression in the brain and muscle of MTKO mice was examined using TrkB Flox F (ACA CAC ACA GTA TAT TTT ACC A) and TrkB Flox R (CAA GAA GTC AGA GAC CAG AGA GA). Cre-5′ (CCT GGA AAA TGC TTC TGT CCG TTT GCC); Cre-3′ (GAG TTG ATA GCT GGC TGG TGG CAG ATG).

Fatty Acid Oxidation Assay

Fatty acid oxidation was measured by determining the production of ^3H_2O from [9,10-^{3}H]palmitate as reported (Chan et al., 2010). Briefly, albumin-bound tritiated palmitate was added to C2C12 myotubes and incubated for 2 hr at 37°C. After incubation, the medium was removed and added to a tube containing cold 10% trichoroacetic acid. The

Author Manuscript Author Manuscript Author Manuscript Author Manuscript

supernatant was then neutralized with NaOH, applied to ion-exchange resin to separate the $^{3}H_{2}O$, and counted by scintillation counting.

Hyperinsulinemic-Euglycemic Clamp

The hyperinsulinemic-euglycemic clamp was performed at the Vanderbilt Mouse Metabolic Phenotyping Center. Catheters were implanted into a carotid artery and a jugular vein of mice for sampling and infusions, respectively, 5 days before the study. Insulin clamps were performed on mice fasted for 5 hr using a modification of the method described by Ayala et al. (2006). [3-^{3}H]Glucose was primed (2.4 μCi) and continuously infused for 90-min equilibration and basal sampling periods (0.04 μCi/min). [3-^{3}H]Glucose was mixed with the nonradioactive glucose infusate (infusate specific activity of 0.4 μCi/mg) during the 2-hr clamp period. Arterial glucose was clamped using a variable rate of glucose (plus trace [3-^{3}H]glucose) infusion, which was adjusted based on the measurement of blood glucose at 10-min intervals. By mixing radioactive glucose with the nonradioactive glucose infused during a clamp, deviations in arterial glucose-specific activity are minimized and steady-state conditions are achieved. Baseline blood or plasma variables were calculated as the mean of values obtained in blood samples collected at −15 and −5 min. At time zero, insulin infusion (2.5 mU/kg of body weight per min) was started and continued for 120 min. Mice received heparinized saline-washed erythrocytes from donors at 5 μl/min to prevent a fall in hematocrit level. Insulin clamps were validated by assessment of blood glucose over time. Blood was taken at 80–120 min for the determination of [3-^{3}H]glucose. Clamp insulin was determined at t = 120 min. At 120 min, 13 μCi of 2[^{14}C]deoxyglucose ([^{14}C]2DG) was administered as an intravenous bolus. Blood was taken at 2–25 min for the determination of [^{14}C]2DG. After the last sample, mice were anesthetized and tissues were freeze-clamped for biochemical analysis. Plasma insulin was determined by ELISA. Radioactivity of [3-^{3}H]glucose and [^{14}C]2DG in plasma samples and [^{14}C]2DG-6-phosphate in tissue samples was determined by liquid scintillation counting.

Body Composition Analysis and Indirect Calorimetry

Body composition and indirect calorimetry analyses were performed at the Vanderbilt Mouse Metabolic Phenotyping Center using Minispec Model mq7.5 (7.5 mHz) (Bruker Instruments) and the Promethion system (Sable Systems), respectively. For indirect calorimetry, mice were individually housed for a week prior to the measurements. Indirect calorimetry was measured for 5 consecutive days. Body composition of mice was assessed before and after the indirect calorimetry measurement.

ADP/ATP Measurement

Cellular ATP and ADP concentrations were measured using the ApoSENSOR ADP/ATP Ratio Bioluminescence Assay Kit (BioVision).

In Vitro AMPK Activity

AMPK was immunoprecipitated from lysed HEK293 cells using anti-AMPKα antibody and Protein A/G agarose (Santa Cruz Biotechnology). The agarose was then washed extensively with lysis buffer and the kinase activity in phosphorylating SAMS peptide was determined

Author Manuscript Author Manuscript Author Manuscript Author Manuscript

as reported (Hardie et al., 2000). Briefly, immunoprecipitated AMPK was stimulated with 7,8-DHF for 30 min at 37°C. A mixture of [γ-^{32}P]ATP, ATP, and SAMS peptide in HEPES buffer was then added to the immunoprecipitated AMPK and incubated for an additional 10 min. The reaction mixture was spotted on Whatman paper. After extensive washing with 1% (v/v) phosphoric acid, the amount of labeled SAMS peptide was determined by scintillation counting.

Adipogenesis

3T3-L1 cells were grown in DMEM with 10% CS. Two days after 100% confluence, the cells were then induced to differentiate into adipocytes by changing the medium to DMEM containing a standard induction cocktail of 10% fetal bovine serum (FBS), 0.5 mM 3-isobutyl-1-methylxanthine, 1 μM dexamethasone, 1.7 μM insulin, and various concentrations of 7,8-DHF. After 48 hr, this medium was replaced with DMEM supplemented with 10% FBS, 1.7 μM insulin, 1 μM ciglitazone, and various concentrations of 7,8-DHF for 48 hr. The cells were then further cultured in DMEM with 10% FBS and various concentrations of 7,8-DHF until assayed. Lipid accumulation was examined by oil red O staining, followed by extraction of the absorbed dye using 100% isopropanol and measurement at 500 nm.

Statistical Analysis

Results were expressed as means ± SEM and were considered significant when $P < 0.05$. Statistical analysis of the data was performed using Student's t test, one-way or two-way ANOVA followed by Tukey's multiple comparison test using the computer program GraphPad Prism (GraphPad Software).

Supplementary Material

Refer to Web version on PubMed Central for supplementary material.

ACKNOWLEDGMENTS

We would like to thank the Emory Integrated Genomic Core for performing the microarray analysis and the Vanderbilt Mouse Metabolic Phenotyping Center (DK059637) for their assistance in performing the hyperinsulinemic-euglycemic clamp assay and metabolic cage study. This work is supported by grants from NIH (NIH DK097092), Oklahoma Center for the Advancement of Science & Technology (OCAST HR14-117) to C.B.C., and NIH DC010204 to K.Y.

REFERENCES

Andero R, Daviu N, Escorihuela RM, Nadal R, Armario A. 7,8-Dihydroxyflavone, a TrkB receptor agonist, blocks long-term spatial memory impairment caused by immobilization stress in rats. Hippocampus. 2012; 22:399–408. [PubMed: 21136519]

Aquila H, Link TA, Klingenberg M. The uncoupling protein from brown fat mitochondria is related to the mitochondrial ADP/ATP carrier. Analysis of sequence homologies and of folding of the protein in the membrane. EMBO J. 1985; 4:2369–2376. [PubMed: 3000775]

Ayala JE, Bracy DP, McGuinness OP, Wasserman DH. Considerations in the design of hyperinsulinemic-euglycemic clamps in the conscious mouse. Diabetes. 2006; 55:390–397. [PubMed: 16443772]

Author Manuscript Author Manuscript Author Manuscript Author Manuscript

Bai Y, Attardi G. The mtDNA-encoded ND6 subunit of mitochondrial NADH dehydrogenase is essential for the assembly of the membrane arm and the respiratory function of the enzyme. EMBO J. 1998; 17:4848–4858. [PubMed: 9707444]

Baker-Andresen D, Flavell CR, Li X, Bredy TW. Activation of BDNF signaling prevents the return of fear in female mice. Learn. Mem. 2013; 20:237–240. [PubMed: 23589089]

Burattini S, Ferri P, Battistelli M, Curci R, Luchetti F, Falcieri E. C2C12 murine myoblasts as a model of skeletal muscle development: morpho-functional characterization. Eur. J. Histochem. 2004; 48:223–233. [PubMed: 15596414]

Camerino C, Zayzafoon M, Rymaszewski M, Heiny J, Rios M, Hauschka PV. Central depletion of brain-derived neurotrophic factor in mice results in high bone mass and metabolic phenotype. Endocrinology. 2012; 153:5394–5405. [PubMed: 23011922]

Cannon B, Nedergaard J. Brown adipose tissue: function and physiological significance. Physiol. Rev. 2004; 84:277–359. [PubMed: 14715917]

Chan CB, Liu X, Jung DY, Jun JY, Luo HR, Kim JK, Ye K. Deficiency of phosphoinositide 3-kinase enhancer protects mice from diet-induced obesity and insulin resistance. Diabetes. 2010; 59:883–893. [PubMed: 20068140]

Cummings DE, Brandon EP, Planas JV, Motamed K, Idzerda RL, McKnight GS. Genetically lean mice result from targeted disruption of the RII beta subunit of protein kinase A. Nature. 1996; 382:622–626. [PubMed: 8757131]

Cuppini R, Sartini S, Agostini D, Guescini M, Ambrogini P, Betti M, Bertini L, Vallasciani M, Stocchi V. Bdnf expression in rat skeletal muscle after acute or repeated exercise. Arch. Ital. Biol. 2007; 145:99–110. [PubMed: 17639782]

del Mar Gonzalez-Barroso M, Pecqueur C, Gelly C, Sanchis D, Alves-Guerra MC, Bouillaud F, Ricquier D, Cassard-Doulcier AM. Transcriptional activation of the human ucp1 gene in a rodent cell line. Synergism of retinoids, isoproterenol, and thiazolidinedione is mediated by a multipartite response element. J. Biol. Chem. 2000; 275:31722–31732. [PubMed: 10921912]

English AW, Liu K, Nicolini JM, Mulligan AM, Ye K. Small-molecule trkB agonists promote axon regeneration in cut peripheral nerves. Proc. Natl. Acad. Sci. USA. 2013; 110:16217–16222. [PubMed: 24043773]

Finkbeiner S, Tavazoie SF, Maloratsky A, Jacobs KM, Harris KM, Greenberg ME. CREB: a major mediator of neuronal neurotrophin responses. Neuron. 1997; 19:1031–1047. [PubMed: 9390517]

Fu Z, Zhang W, Zhen W, Lum H, Nadler J, Bassaganya-Riera J, Jia Z, Wang Y, Misra H, Liu D. Genistein induces pancreatic beta-cell proliferation through activation of multiple signaling pathways and prevents insulin-deficient diabetes in mice. Endocrinology. 2010; 151:3026–3037. [PubMed: 20484465]

Funakoshi H, Frisen J, Barbany G, Timmusk T, Zachrisson O, Verge VM, Persson H. Differential expression of mRNAs for neurotrophins and their receptors after axotomy of the sciatic nerve. J. Cell Biol. 1993; 123:455–465. [PubMed: 8408225]

Gray J, Yeo GS, Cox JJ, Morton J, Adlam AL, Keogh JM, Yanovski JA, El Gharbawy A, Han JC, Tung YC, et al. Hyperphagia, severe obesity, impaired cognitive function, and hyperactivity associated with functional loss of one copy of the brain-derived neurotrophic factor (BDNF) gene. Diabetes. 2006; 55:3366–3371. [PubMed: 17130481]

Gupta VK, You Y, Li JC, Klistorner A, Graham SL. Protective effects of 7,8-dihydroxyflavone on retinal ganglion and RGC-5 cells against excitotoxic and oxidative stress. J. Mol. Neurosci. 2013; 49:96–104. [PubMed: 23054592]

Han DH, Nolte LA, Ju JS, Coleman T, Holloszy JO, Semenkovich CF. UCP-mediated energy depletion in skeletal muscle increases glucose transport despite lipid accumulation and mitochondrial dysfunction. Am. J. Physiol. Endocrinol. Metab. 2004; 286:E347–353. [PubMed: 14613927]

Hardie DG, Salt IP, Davies SP. Analysis of the role of the AMP-activated protein kinase in the response to cellular stress. Methods Mol. Biol. 2000; 99:63–74. [PubMed: 10909077]

Huang EJ, Reichardt LF. Neurotrophins: roles in neuronal development and function. Annu. Rev. Neurosci. 2001; 24:677–736. [PubMed: 11520916]

Author Manuscript Author Manuscript Author Manuscript Author Manuscript

Jang SW, Liu X, Yepes M, Shepherd KR, Miller GW, Liu Y, Wilson WD, Xiao G, Blanchi B, Sun YE, Ye K. A selective TrkB agonist with potent neurotrophic activities by 7,8-dihydroxyflavone. Proc. Natl. Acad. Sci. USA. 2010; 107:2687–2692. [PubMed: 20133810]

Jiang M, Peng Q, Liu X, Jin J, Hou Z, Zhang J, Mori S, Ross CA, Ye K, Duan W. Small-molecule TrkB receptor agonists improve motor function and extend survival in a mouse model of Huntington's disease. Hum. Mol. Genet. 2013; 22:2462–2470. [PubMed: 23446639]

Johnson RA, Lam M, Punzo AM, Li H, Lin BR, Ye K, Mitchell GS, Chang Q. 7,8-dihydroxyflavone exhibits therapeutic efficacy in a mouse model of Rett syndrome. J. Appl. Phys. (1985). 2012; 112:704–710.

Keipert S, Ost M, Chadt A, Voigt A, Ayala V, Portero-Otin M, Pamplona R, Al-Hasani H, Klaus S. Skeletal muscle uncoupling-induced longevity in mice is linked to increased substrate metabolism and induction of the endogenous antioxidant defense system. Am. J. Physiol. Endocrinol. Metab. 2013; 304:E495–E506. [PubMed: 23277187]

Kernie SG, Liebl DJ, Parada LF. BDNF regulates eating behavior and locomotor activity in mice. EMBO J. 2000; 19:1290–1300. [PubMed: 10716929]

Klaus S, Rudolph B, Dohrmann C, Wehr R. Expression of un-coupling protein 1 in skeletal muscle decreases muscle energy efficiency and affects thermoregulation and substrate oxidation. Physiol. Genomics. 2005; 21:193–200. [PubMed: 15687481]

Li B, Nolte LA, Ju JS, Han DH, Coleman T, Holloszy JO, Semenkovich CF. Skeletal muscle respiratory uncoupling prevents diet-induced obesity and insulin resistance in mice. Nat. Med. 2000; 6:1115–1120. [PubMed: 11017142]

Liu X, Chan CB, Jang SW, Pradoldej S, Huang J, He K, Phun LH, France S, Xiao G, Jia Y, et al. A synthetic 7,8-dihydroxyflavone derivative promotes neurogenesis and exhibits potent antidepressant effect. J. Med. Chem. 2010; 53:8274–8286. [PubMed: 21073191]

Liu X, Qi Q, Xiao G, Li J, Luo HR, Ye K. O-methylated metabolite of 7,8-dihydroxyflavone activates TrkB receptor and displays anti-depressant activity. Pharmacology. 2013; 91:185–200. [PubMed: 23445871]

Matsuzaka T, Shimano H, Yahagi N, Kato T, Atsumi A, Yamamoto T, Inoue N, Ishikawa M, Okada S, Ishigaki N, et al. Crucial role of a long-chain fatty acid elongase, Elovl6, in obesity-induced insulin resistance. Nat. Med. 2007; 13:1193–1202. [PubMed: 17906635]

Matthews VB, Astrom MB, Chan MH, Bruce CR, Krabbe KS, Prelovsek O, Akerstrom T, Yfanti C, Broholm C, Mortensen OH, et al. Brain-derived neurotrophic factor is produced by skeletal muscle cells in response to contraction and enhances fat oxidation via activation of AMP-activated protein kinase. Diabetologia. 2009; 52:1409–1418. [PubMed: 19387610]

Monteggia LM, Luikart B, Barrot M, Theobold D, Malkovska I, Nef S, Parada LF, Nestler EJ. Brain-derived neurotrophic factor conditional knockouts show gender differences in depression-related behaviors. Biol. Psychiatry. 2007; 61:187–197. [PubMed: 16697351]

Nakagawa T, Tsuchida A, Itakura Y, Nonomura T, Ono M, Hirota F, Inoue T, Nakayama C, Taiji M, Noguchi H. Brain-derived neurotrophic factor regulates glucose metabolism by modulating energy balance in diabetic mice. Diabetes. 2000; 49:436–444. [PubMed: 10868966]

Neschen S, Katterle Y, Richter J, Augustin R, Scherneck S, Mirhashemi F, Schurmann A, Joost HG, Klaus S. Uncoupling protein 1 expression in murine skeletal muscle increases AMPK activation, glucose turnover, and insulin sensitivity in vivo. Physiol. Genomics. 2008; 33:333–340. [PubMed: 18349383]

Numakawa T, Suzuki S, Kumamaru E, Adachi N, Richards M, Kunugi H. BDNF function and intracellular signaling in neurons. Histol. Histopathol. 2010; 25:237–258. [PubMed: 20017110]

Pelleymounter MA, Cullen MJ, Wellman CL. Characteristics of BDNF-induced weight loss. Exp. Neurol. 1995; 131:229–238. [PubMed: 7534721]

Poduslo JF, Curran GL. Permeability at the blood-brain and blood-nerve barriers of the neurotrophic factors: NGF, CNTF, NT-3, BDNF. Brain Res. Mol. Brain Res. 1996; 36:280–286. [PubMed: 8965648]

Reich M, Liefeld T, Gould J, Lerner J, Tamayo P, Mesirov JP. GenePattern 2.0. Nat. Genet. 2006; 38:500–501. [PubMed: 16642009]

Author Manuscript Author Manuscript Author Manuscript Author Manuscript

Rim JS, Kozak LP. Regulatory motifs for CREB-binding protein and Nfe2l2 transcription factors in the upstream enhancer of the mitochondrial uncoupling protein 1 gene. J. Biol. Chem. 2002; 277:34589–34600. [PubMed: 12084707]

Rios M. BDNF and the central control of feeding: accidental bystander or essential player? Trends Neurosci. 2013; 36:83–90. [PubMed: 23333344]

Shelton DL, Sutherland J, Gripp J, Camerato T, Armanini MP, Phillips HS, Carroll K, Spencer SD, Levinson AD. Human trks: molecular cloning, tissue distribution, and expression of extracellular domain immunoadhesins. J. Neurosci. 1995; 15:477–491. [PubMed: 7823156]

Spencer JL, Waters EM, Milner TA, McEwen BS. Estrous cycle regulates activation of hippocampal Akt, LIM kinase, and neurotrophin receptors in C57BL/6 mice. Neuroscience. 2008; 155:1106–1119. [PubMed: 18601981]

Sztalryd C, Xu G, Dorward H, Tansey JT, Contreras JA, Kimmel AR, Londos C. Perilipin A is essential for the translocation of hormone-sensitive lipase during lipolytic activation. J. Cell Biol. 2003; 161:1093–1103. [PubMed: 12810697]

Tapley P, Lamballe F, Barbacid M. K252a is a selective inhibitor of the tyrosine protein kinase activity of the trk family of oncogenes and neurotrophin receptors. Oncogene. 1992; 7:371–381. [PubMed: 1312698]

Tseng YH, Kokkotou E, Schulz TJ, Huang TL, Winnay JN, Taniguchi CM, Tran TT, Suzuki R, Espinoza DO, Yamamoto Y, et al. New role of bone morphogenetic protein 7 in brown adipogenesis and energy expenditure. Nature. 2008; 454:1000–1004. [PubMed: 18719589]

Tsuchida A, Nonomura T, Ono-Kishino M, Nakagawa T, Taiji M, Noguchi H. Acute effects of brain-derived neurotrophic factor on energy expenditure in obese diabetic mice. Int. J. Obes. Relat. Metab. Disord. 2001; 25:1286–1293. [PubMed: 11571589]

Uluc K, Kendigelen P, Fidan E, Zhang L, Chanana V, Kintner D, Akture E, Song C, Ye K, Sun D, et al. TrkB receptor agonist 7, 8 dihydroxyflavone triggers profound gender-dependent neuroprotection in mice after perinatal hypoxia and ischemia. CNS Neurol. Disord. Drug Targets. 2013; 12:360–370. [PubMed: 23469848]

Unger TJ, Calderon GA, Bradley LC, Sena-Esteves M, Rios M. Selective deletion of Bdnf in the ventromedial and dorsomedial hypothalamus of adult mice results in hyperphagic behavior and obesity. J. Neurosci. 2007; 27:14265–14274. [PubMed: 18160634]

Wang C, Bomberg E, Billington CJ, Levine AS, Kotz CM. Brain-derived neurotrophic factor (BDNF) in the hypothalamic ventromedial nucleus increases energy expenditure. Brain Res. 2010; 1336:66–77. [PubMed: 20398635]

Yeo GS, Connie Hung CC, Rochford J, Keogh J, Gray J, Sivaramakrishnan S, O'Rahilly S, Farooqi IS. A de novo mutation affecting human TrkB associated with severe obesity and developmental delay. Nat. Neurosci. 2004; 7:1187–1189. [PubMed: 15494731]

Yu Q, Chang Q, Liu X, Wang Y, Li H, Gong S, Ye K, Lin X. Protection of spiral ganglion neurons from degeneration using small-molecule TrkB receptor agonists. J. Neurosci. 2013; 33:13042–13052. [PubMed: 23926258]

Zhang Z, Liu X, Schroeder JP, Chan CB, Song M, Yu SP, Weinshenker D, Ye K. 7,8-Dihydroxyflavone prevents synaptic loss and memory deficits in a mouse model of Alzheimer's disease. Neuropsychopharmacology. 2013; 39:638–650. [PubMed: 24022672]

Zhou Y, Jiang L, Rui L. Identification of MUP1 as a regulator for glucose and lipid metabolism in mice. J. Biol. Chem. 2009; 284:11152–11159. [PubMed: 19258313]

Author Manuscript Author Manuscript Author Manuscript Author Manuscript

Highlights

- 7,8-DHF reduces body weight gain in DIO mice
- 7,8-DHF acts on the skeletal muscle to reduce diet-induced body weight increase
- 7,8-DHF increases energy expenditure of muscle cells through UCP1 and AMPK

Author Manuscript Author Manuscript Author Manuscript Author Manuscript

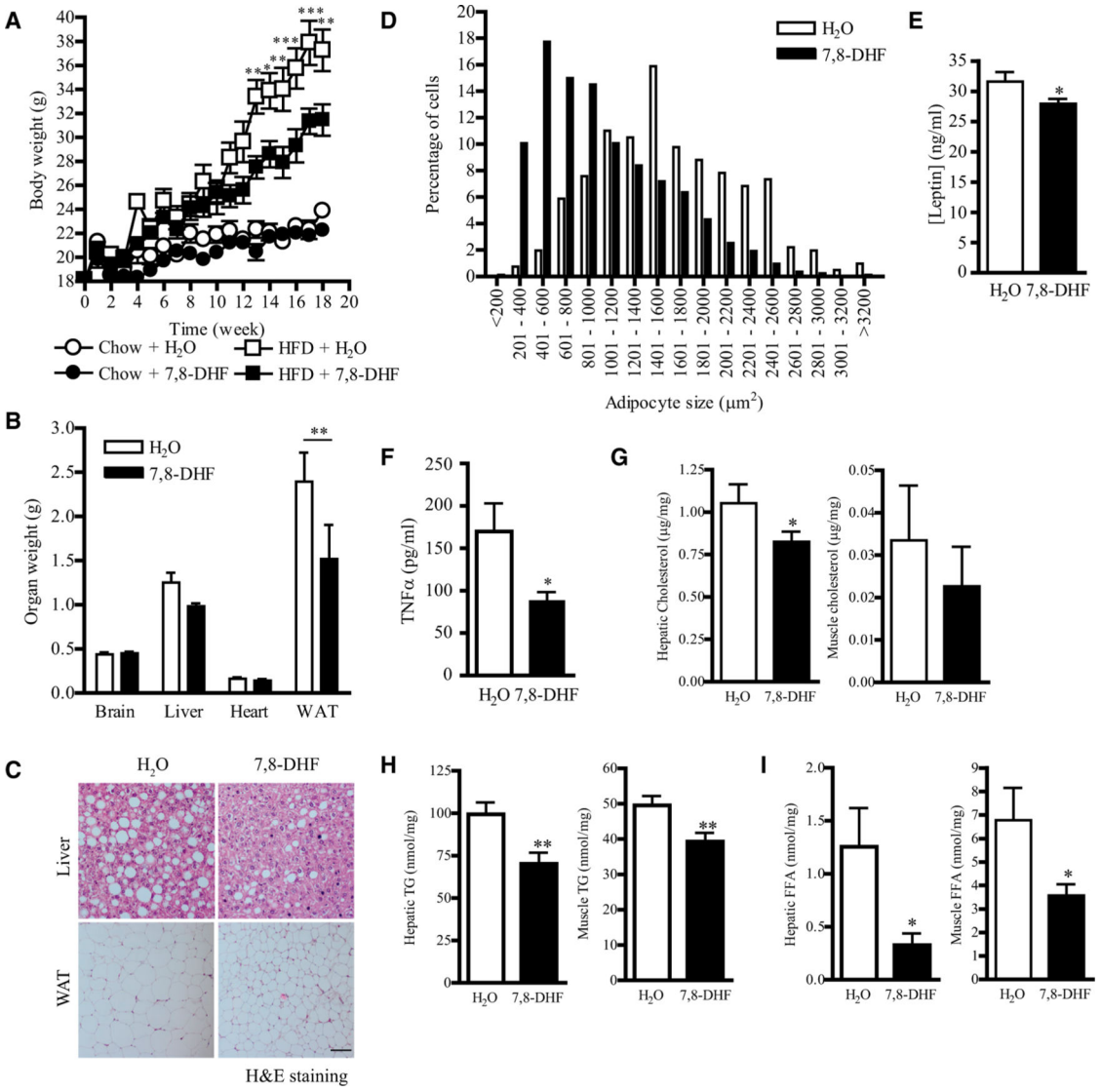

Figure 1. 7,8-DHF-Treated Female Mice Are Resistant to Diet-Induced Obesity

(A) Growth curve of 8-week-old female mice fed with different combinations of diets (***P* < 0.01, ***P* < 0.001, two-way ANOVA versus the same diet feeding, n = 8–10).

(B) Organ weight of female mice that have been fed with HFD and 7,8-DHF for 20 weeks (***P* < 0.01, Student's t test, n = 5).

(C) Pictures of H&E staining of inguinal WAT and liver sections from female mice that have been fed with HFD and 7,8-DHF for 20 weeks. Representative results of four different mice from each treatment are shown. Scale bar represents 50 mm.

(D) Adipocyte size of inguinal fat pad isolated from female mice that have been fed with HFD and 7,8-DHF for 20 weeks (n = 4).

(E) Circulating leptin concentration in female mice that have been fed with HFD and 7,8-DHF for 20 weeks (**P* < 0.05, Student's t test, n = 6).

(F) Circulating TNFα concentration in female mice that have been fed with HFD and 7,8-DHF for 20 weeks (**P* < 0.05, Student's t test, n = 6).

Author Manuscript Author Manuscript Author Manuscript Author Manuscript

(G) Tissue cholesterol content in female mice that have been fed with HFD and 7,8-DHF for 20 weeks (*$P < 0.05$, Student's t test, n = 6).
(H) Tissue TG content in female mice that have been fed with HFD and 7,8-DHF for 20 weeks (**$P < 0.01$, Student's t test, n = 6).
(I) Tissue FFA content in female mice that have been fed with HFD and 7,8-DHF for 20 weeks (**$P < 0.01$, Student's t test, n = 6). See also Figures S1 and S2. Results were presented as means ± SEM.

Author Manuscript Author Manuscript Author Manuscript Author Manuscript

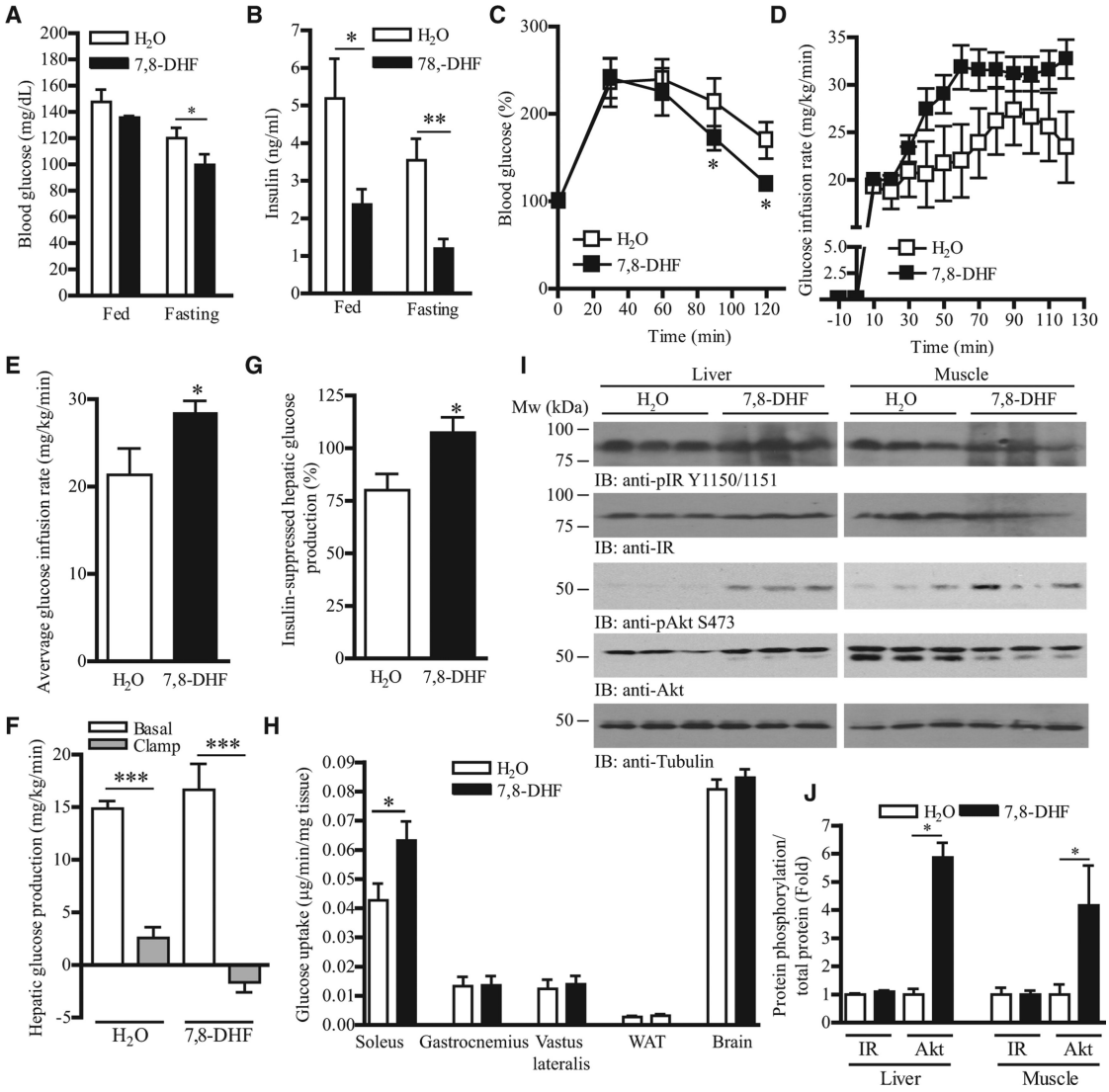

Figure 2. Alleviated Obesity-Induced Insulin Resistance in 7,8-DHF-Treated Female Mice

(A) Blood glucose concentration in female mice that have been fed with HFD and 7,8-DHF for 20 weeks (*P < 0.05, Student's t test, n = 6).

(B) Circulating insulin concentration in female mice that have been fed with HFD and 7,8-DHF for 20 weeks (*P < 0.05, **P < 0.01, Student's t test, n = 6).

(C) Glucose tolerance test in female mice that have been fed with HFD and 7,8-DHF for 20 weeks (*P < 0.05, two-way ANOVA, n = 5).

(D) Glucose infusion rate in female mice that have been fed with HFD and 7,8-DHF for 20 weeks during the hyperinsulinemic-euglycemic clamp experiment (n = 6).

(E) Average glucose infusion rate during the hyperinsulinemic-euglycemic clamp experiment (*P < 0.05, Student's t test, n = 6).

(F) Hepatic glucose production of female mice that have been fed with HFD and 7,8-DHF for 20 weeks during the hyperinsulinemic-euglycemic clamp (***P < 0.001, Student's t test, n = 6).

Author Manuscript Author Manuscript Author Manuscript Author Manuscript

(G) Percentage of insulin-suppressed glucose production from liver during the hyperinsulinemic-euglycemic clamp (*P < 0.05, Student's t test, n = 6).
(H) Glucose uptake in various tissues during the hyperinsulinemic-euglycemic clamp (*P < 0.001, Student's t test, n = 5).
(I) Enhanced insulin-induced signaling in female mice that have been fed with HFD and 7,8-DHF for 20 weeks. The phosphorylations of IR (first panel) and Akt (third panel) were determined using specific antibodies as indicated. The expression of total IR (second panel) and Akt (fourth panel) were determined to show equal loading.
(J) Quantification of the band intensity shown in (I) (*P < 0.05, Student t test, n = 3). Results were presented as means ± SEM.

Author Manuscript Author Manuscript Author Manuscript Author Manuscript

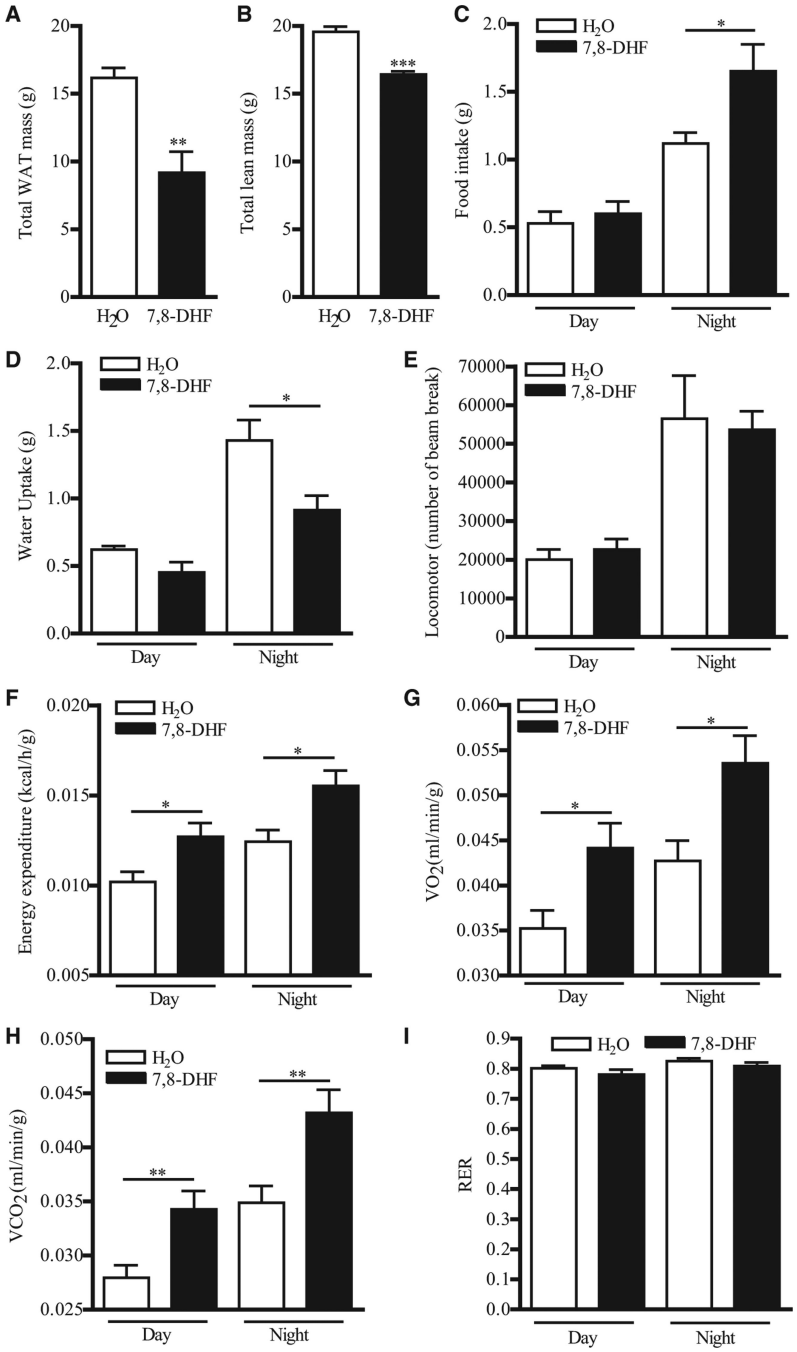

Figure 3. 7,8-DHF Treatment Increases Energy Expenditure in HFD-Fed Female Mice

(A) Total fat mass of female mice that have been fed with HFD and 7,8-DHF for 20 weeks as measured by indirect calorimetry (**P < 0.01, Student's t test, n = 6).

(B) Total lean mass of female mice that have been fed with HFD and 7,8-DHF for 20 weeks measured by indirect calorimetry (***P < 0.001, Student's t test, n = 6).

(C) Food intake of female mice that have been fed with HFD and 7,8-DHF for 20 weeks during the metabolic cage measurement (*P < 0.05, Student's t test, n = 6).

Author Manuscript Author Manuscript Author Manuscript Author Manuscript

(D) Water uptake of female mice that have been fed with HFD and 7,8-DHF for 20 weeks during the metabolic cage measurement (*P < 0.05, Student's t test, n = 6).
(E) Locomotor activity of female mice that have been fed with HFD and 7,8-DHF for 20 weeks during the metabolic cage measurement (n = 6).
(F) Energy expenditure of female mice that have been fed with HFD and 7,8-DHF for 20 weeks during the metabolic cage measurement (*P < 0.05, Student's t test, n = 6).
(G) Oxygen consumption of female mice that have been fed with HFD and 7,8-DHF for 20 weeks during the metabolic cage measurement (*P < 0.05, Student's t test, n = 6).
(H) Carbon dioxide production from female mice that have been fed with HFD and 7,8-DHF for 20 weeks during the metabolic cage measurement (**P < 0.01, Student's t test, n = 6).
(I) RER of female mice that have been fed with HFD and 7,8-DHF for 20 weeks during the metabolic cage measurement (n = 6).
See also Figure S3. Results were presented as means ± SEM.

Author Manuscript Author Manuscript Author Manuscript Author Manuscript

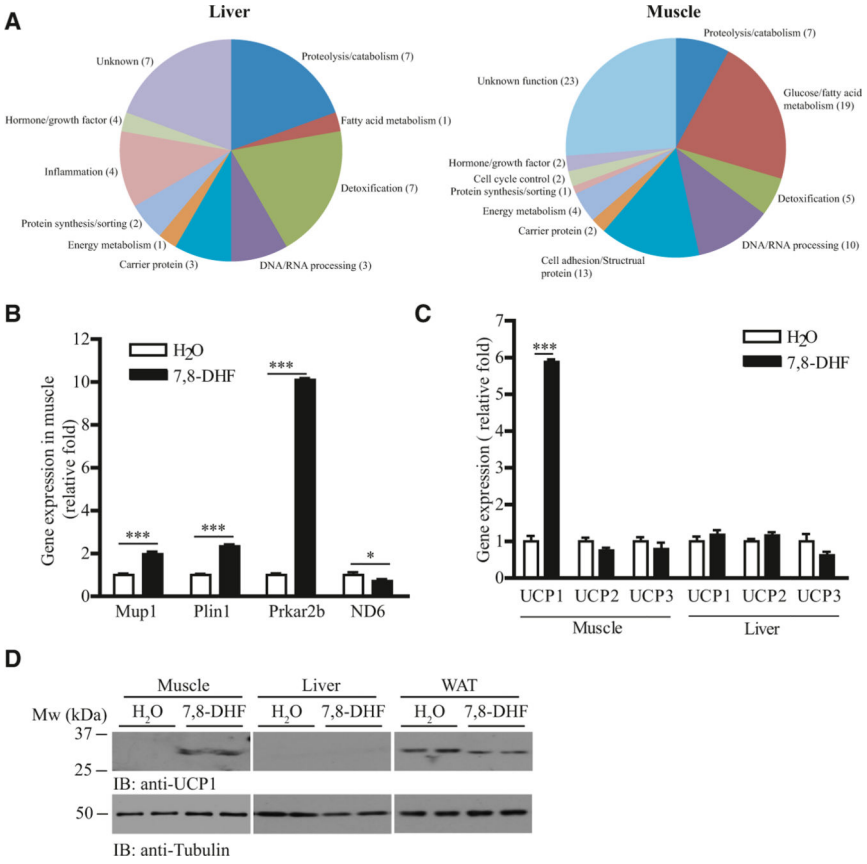

Figure 4. Gene Expression and Signaling Analyses in 7,8-DHF-Treated Female Mice

(A) Classification of 7,8-DHF-induced genes in the liver and hindlimb muscle isolated from female mice that have been fed with HFD and 7,8-DHF for 20 weeks.

(B) Expression of representative skeletal muscle genes in female mice that have been fed with HFD and 7,8-DHF for 20 weeks as measured by real-time PCR analysis (*$P < 0.05$, ***$P < 0.01$, Student's t test, n = 3).

(C) Expression of various UCP isoforms in the skeletal muscle of female mice that have been fed with HFD and 7,8-DHF for 20 weeks (***$P < 0.01$, Student's t test, n = 3).

(D) Expression of UCP1 in various tissues isolated from female mice that have been fed with HFD and 7,8-DHF for 20 weeks.

Results were presented as means ± SEM.

Author Manuscript Author Manuscript Author Manuscript Author Manuscript

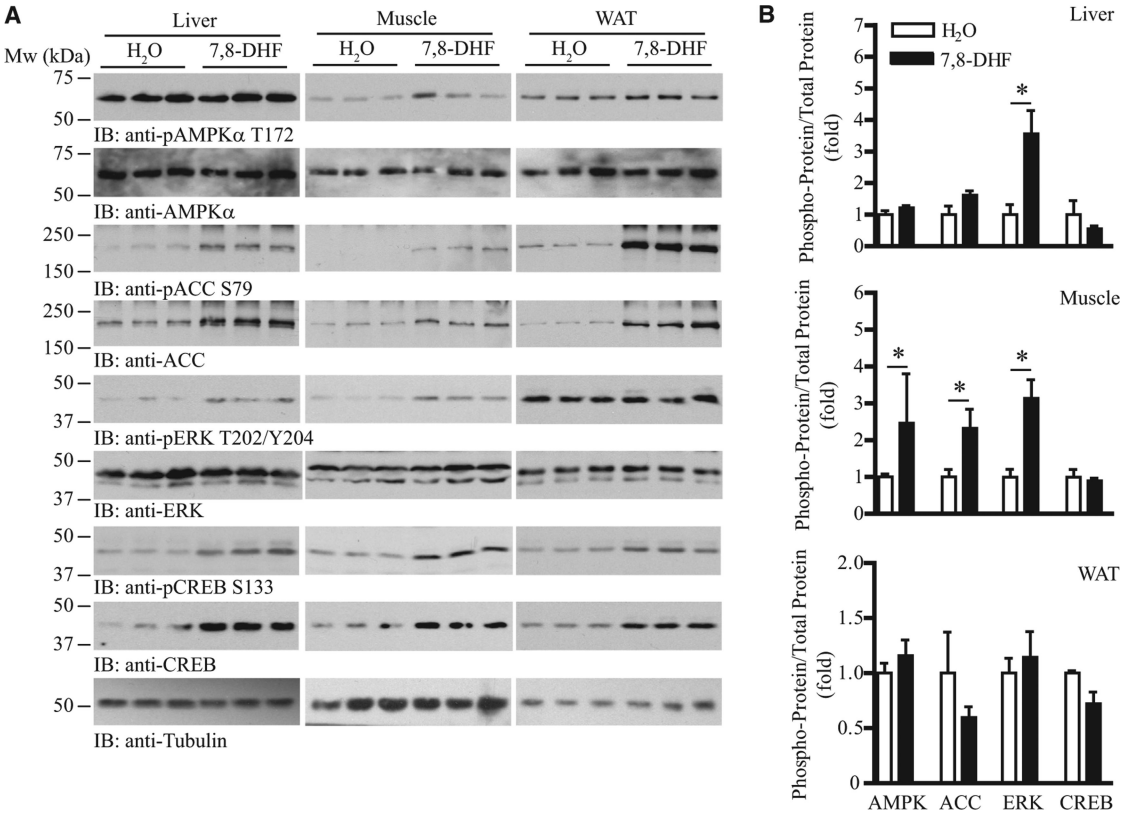

Figure 5. 7,8-DHF Treatment Enhances AMPK/ACC Signaling in HFD-Fed Female Mice

(A) Immunoblot analysis of various tissues isolated from female mice that have been treated with 7,8-DHF for 20 weeks.

(B) Quantification of the protein phosphorylation shown in (A) (*$P < 0.05$, Student's t test, n = 3).

See also Figure S4. Results were presented as means ± SEM.

Author Manuscript Author Manuscript Author Manuscript Author Manuscript

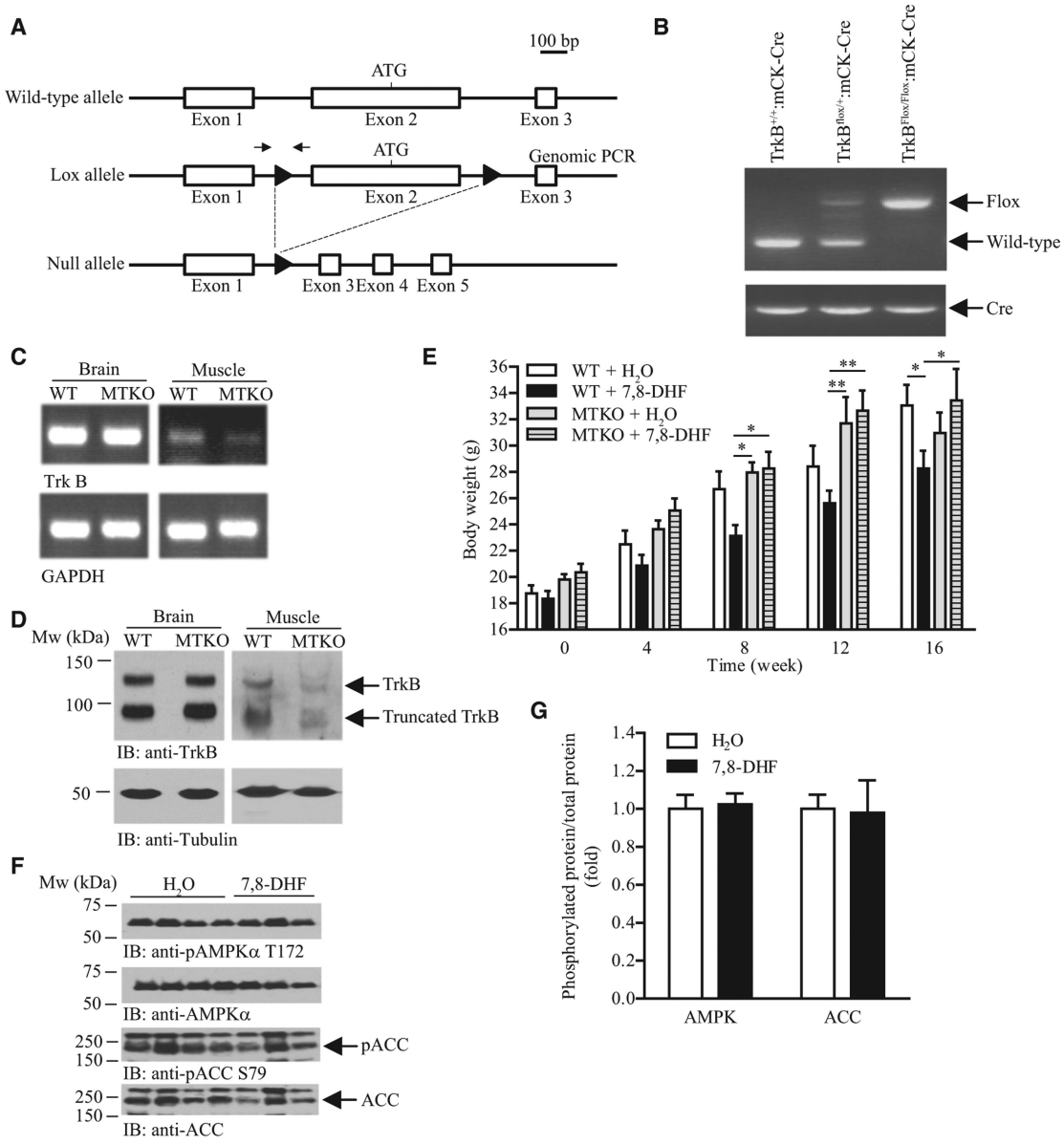

Figure 6. Muscle TrkB Is the Major Target of 7,8-DHF to Prevent Diet-Induced Obesity

(A) A schematic representation of mouse TrkB deletion using loxP/Cre recombination. The location of loxP sites were marked as solid triangles. Locations of the primers used in the genomic PCR are indicated by the arrows.

(B) Deletion of TrkB in MTKO mice. Genomic DNA were isolated from the tail tip of female mice and used to perform PCR.

(C) Reduced TrkB expression in the skeletal muscle of MTKO mice. Total RNA was isolated from various tissues of female MTKO mice and used to generate cDNA. PCR was then performed to determine TrkB expression. Expression of GAPDH was also tested as control.

(D) MTKO mice have less TrkB protein in the skeletal muscle cell lysates were prepared from various tissues of female MTKO mice and the amount of TrkB proteins was examined using immunoblotting.

Author Manuscript Author Manuscript Author Manuscript Author Manuscript

(E) Growth curve of 8-week-old female mice fed with HFD and 7,8-DHF in the drinking water (0.16 mg/ml) (*P < 0.05, **P < 0.01, two-way ANOVA, n = 7–10).
(F) Immunoblotting analysis of AMPK and ACC phosphorylation in muscle isolated from female MTKO mice that have been treated with 7,8-DHF for 16 weeks.
(G) Quantification of the protein phosphorylation shown in (F) (n = 3).
Results were presented as means ± SEM.

Author Manuscript Author Manuscript Author Manuscript Author Manuscript

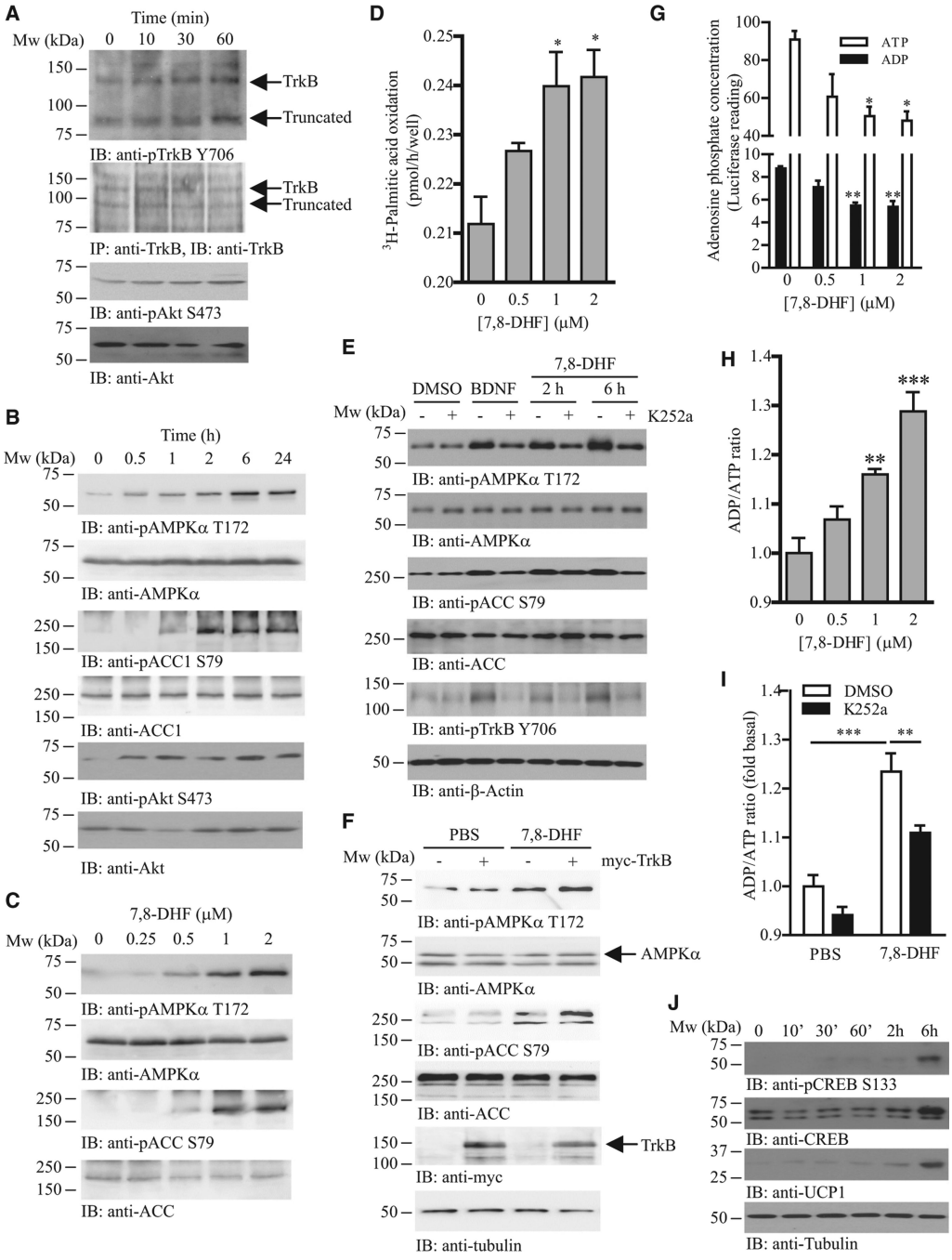

Figure 7. 7,8-DHF Treatment Enhances Lipid Oxidation, ADP/ATP Ratio, and UCP1 Expression in Cultured Muscle Cells

(A) 7,8-DHF induces TrkB phosphorylation in muscle cells. Differentiated C2C12 myotubes were stimulated with 7,8-DHF (1 μM) for various time intervals as indicated. Cell lysates were then collected and the phosphorylation of TrkB (first panel) and Akt (third panel) was examined. Total TrkB (second panel) and Akt (fourth panel) were also verified.

(B) 7,8-DHF activates AMPK and ACC in muscle cells. Differentiated C2C12 myotubes were stimulated with 7,8-DHF (1 μM) for various time intervals as indicated. Cell lysates were then collected and the phosphorylation of AMPK (first panel), ACC (third panel), and

Author Manuscript Author Manuscript Author Manuscript Author Manuscript

Akt (fifth panel) was examined. Total AMPK (second panel), ACC (fourth panel), and Akt (sixth panel) were also verified.

(C) Dose-dependent induction of AMPK and ACC phosphorylations in muscle cells after 7,8-DHF stimulation. Differentiated C2C12 myotubes were stimulated with 7,8-DHF at various concentrations for 24 hr. Cell lysates were then collected and the phosphorylation of AMPK (first panel) and ACC (third panel) was examined. Total AMPK (second panel) and ACC (fourth panel) were also verified.

(D) 7,8-DHF increases lipid oxidation in cultured muscle cells. Differentiated C2C12 myotubes were stimulated with 7,8-DHF at various concentrations for 24 hr, and the palmitic acid oxidation rate was then measured (*$P < 0.05$, one-way ANOVA versus control, n = 3).

(E) Inhibition of TrkB abolishes 7,8-DHF or BDNF-induced AMPK activation. Differentiated C2C12 myotubes were incubated with TrkB kinase inhibitor K252a (10 nM) for 1 hr followed by BDNF (100 ng/ml) for 1 hr or 7,8-DHF (1 μM) for 2 or 6 hr. Cell lysates were then collected and the phosphorylation of AMPK (first panel), ACC (third panel), and TrkB (fifth panel) was examined. Total AMPK (second panel), ACC (fourth panel), and actin (sixth panel) were also verified.

(F) Overexpression of TrkB augments 7,8-DHF-induced AMPK activity. Differentiated C2C12 myotubes were transfected with control or myc-TrkB plasmids followed by 7,8-DHF (1 μM) for 24 hr. Cell lysates were then collected and the phosphorylation of AMPK (first panel) and ACC (third panel) was examined. Total AMPK (second panel) and ACC (fourth panel) were also verified.

(G) 7,8-DHF stimulation reduces cellular ADP and ATP concentration. Differentiated C2C12 myotubes were stimulated with 7,8-DHF at various concentrations for 24 hr. Cell lysates were collected and the cellular concentration of ADP and ATP was then measured (*$P < 0.05$ versus control, one-way ANOVA, n = 3).

(H) 7,8-DHF stimulation increases the cellular ADP/ATP ratio. Differentiated C2C12 myotubes were stimulated with 7,8-DHF at various concentrations for 24 hr. Cell lysates were collected and the cellular concentration of ADP and ATP was then measured (*$P < 0.05$, **$P < 0.01$ versus control, one-way ANOVA, n = 3).

(I) Inhibition of TrkB kinase suppresses the 7,8-DHF-elevated ADP/ATP ratio. Differentiated C2C12 myotubes were incubated with K252a (10 nM) for 1 hr followed by 7,8-DHF (1 μM) for 24 hr. Cell lysates were collected and the cellular concentration of ADP and ATP was then measured (**$P < 0.01$, ***$P < 0.001$, two-way ANOVA, n = 6).

(J) 7,8-DHF increases UCP1 expression in muscle cells. Differentiated C2C12 myotubes were stimulated with 7,8-DHF (1 μM) for various time intervals as indicated. Cell lysates were then collected and the phosphorylation of CREB (first panel) was examined. Total CREB (second panel), UCP1 (third panel), and tubulin (fourth panel) were also verified. See also Figure S5.

Results were presented as means ± SEM.